Envelope Computation in the Plane by Approximate Implicitization

Tino Schulz
Johannes Kepler University of Linz, Austria
tino.schulz@jku.at

Bert Jüttler
Johannes Kepler University of Linz, Austria
bert.juettler@jku.at

Abstract

Given a rational family of planar rational curves in a certain region of interest, we are interested in computing an implicit representation of the envelope. The points of the envelope correspond to the zero set of a function (which represents the envelope condition) in the parameter space combining the curve parameter and the motion parameter. We analyze the connection of this function to the implicit equation of the envelope. This connection enables us to use approximate implicitization for computing the (exact or approximate) implicit representation of the envelope. Based on these results, we formulate an algorithm for computing a piecewise algebraic approximation of low degree and illustrate its performance by several examples.

1 Introduction

The concept of an *envelope*, which is a curve or surface that touches all members of a given family of curves or surfaces, is useful in a variety of applications. In the theory of gearings, envelopes are used to find matching pairs of tooth flanks. In robotics, they are strongly related to the problem of collision detection, due to the close connection of the envelope and the swept volume of a moving solid. Furthermore, envelopes are also of great interest in geometrical optics and NC machining (caustics, path planning) and in Computer-Aided Design (offset curves and surfaces).

Envelopes of curves and surfaces and methods for computing them are discussed in the classical literature from kinematics and differential geometry, cf. [7, 19]. A survey on the topic is given in a paper by Pottmann and Peternell [22]. Abdel-Malek et al. [1] present several approaches for computing swept volumes. An algorithm for computing a boundary representation of swept volumes generated by moving free-form surfaces is presented and discussed in [21].

Special classes of moving surfaces have been studied in more detail. Kim et al. [18] consider swept volumes of moving polyhedra and Flaquer et al. [14] study envelopes of moving quadrics. In a recent paper, Rabl et al. [23] analyze envelopes of moving surfaces which are characterized by a special form of their support function.

The envelope of a rational family of rational curves is generally not rational and its implicit representation is usually of high degree (compared to the degrees of the family). In particular, this is true for *offsets*, which form an important subclass of envelopes. The offset of a curve can be obtained as the envelope of the family of circles with fixed radius which move along the curve. It is well known that the class of algebraic curves and surfaces is closed with respect to the offsetting.

Due to their technical importance, the construction and analysis of offset curves has attracted the attention of many researchers from fields of geometric design, algebraic geometry and symbolic computation. In particular, a substantial number of publications discusses curves and surfaces with rational offsets, see [13] and the references cited therein. The existing literature also includes results concerning offsets of general rational curves. For instance, the implicit equation of the offset curves was shown to be useful for analyzing of topological changes of offset curves, see [2, 3, 4, 24].

Due to its potentially high degree, it is difficult to compute the implicit equation of general envelopes. In order to address this difficulty, we propose to use the technique of *approximate implicitization* for envelope computation in this paper.

Given a parametric description of a curve (or surface), the process of finding the implicit description is called *implicitization*. In the case of a rational parametrization, this conversion is always possible, and the result is an algebraic hypersurface (curve in 2D or surface in 3D), represented as the zero set of a polynomial (see [25, 27]). Several techniques for solving the implicitization problem are available, e.g. Gröbner bases, moving curves/surfaces, or methods based on resultants (cf.[6, 12] and [17]). While planar curves can be handled efficiently with these approaches, their application to surfaces is problematic due to the increased computational complexity. in practice, the use of exact methods for implicitization is only reasonable for surfaces of low degree. Furthermore, the variety provided by the exact implicitization may contain branches and self-intersections that the user would have liked to avoid for certain reasons.

The idea of *approximate implicitization* [8] is to generate an approximation (of low degree) of the exact algebraic representation, which represents the shape of the given curve or surface in the region of interest. Using approximate implicitization it is possible to avoid the difficulties associated with the exact method.

In this paper we will restrict ourselves to the case of a family of planar, rational curves, following the approach introduced by Dokken (cf. [8, 10]). A comparative benchmarking of this technique and of other methods for approximate implicitization may be found in [28] and [31]. Since we are aiming at a local (rather than a global) approximation and on numerical evaluation, we will mainly use the weak formulation of approximate implicitization [9, 11]. It will be shown that the algebraic error of the approximation of the envelope is bounded in a similar way as in the original approach.

This paper is organized as follows. The next two sections recall the concepts of approximate implicitization and envelope computation, respectively. The fourth section introduces the combination of both concepts. Based on these results, we present an algorithm for computing a piecewise, algebraic approximation of a family of rational curves in Section 5. Moreover, several examples will illustrate its performance. Finally we conclude this paper.

2 Approximate implicitization

We recall the classical version of approximate implicitization (AI) and its weak formulation. We also give an outline of how to deal with interpolation constraints in this framework. See [8, 9, 10, 11] for additional details.

2.1 Dokken's first method

Consider a segment of a planar rational parametric curve $s \mapsto \mathbf{p}(s)$, $s \in I$, of degree n, where the compact interval $I \subset \mathbb{R}$ is the parameter domain. We assume that this curve segment is contained in a bounded open subset $\Omega \subset \mathbb{R}^2$, which we call the region of interest.

In order to approximate $\mathbf{p}(s)$, $s \in I$, by an algebraic curve, which is defined as the zero set

$$q^{-1}(0) = \{\mathbf{p} \in \Omega : \; q(\mathbf{p}) = 0\} \tag{1}$$

of a bivariate polynomial $q : \mathbb{R}^2 \to \mathbb{R}$ of degree m, we consider the composition

$$(q \circ \mathbf{p})(s) = q(\mathbf{p}(s)). \tag{2}$$

The polynomial q has a representation of the form

$$q(\mathbf{x}) = \sum_{i=1}^{\binom{m+2}{2}} \beta_i(\mathbf{x}) c_i = \mathbf{c}^T \beta(\mathbf{x}) \tag{3}$$

where the functions β_i are a basis of the space of bivariate polynomials of maximum degree m and the $c_i \in \mathbb{R}$ are the coefficients with respect to it. We collect the coefficients in the coefficient vector $\mathbf{c}$ of q and the basis functions in another vector $\beta(\mathbf{x})$.

The first approach to approximate implicitization is based on a factorization of the composition (2),

$$(q \circ \mathbf{p})(s) = q(\mathbf{p}(s)) = (\mathbf{D}\mathbf{c})^T \alpha(s), \tag{4}$$

where the vector $\alpha(s) = (\alpha_0(s), \ldots \alpha_{mn}(s))^T$ contains a basis of the polynomials of maximum degree mn in s, which is non-negative and forms a partition of unity on I. For instance, one may take the Bernstein polynomials on the interval I. The matrix $\mathbf{D}$, which is determined by the given curve and by the chosen basis α, has mn rows and $\binom{m+2}{2}$ columns.

In order to eliminate the parameter s (and hence to implicitize the given curve), Dokken considers the norms of the vectors and matrices in (4). For all $s \in I$ we have that

$$\sum_i (\alpha_i(s))^2 \leq \sum_i \alpha_i(s) = 1, \tag{5}$$

hence $\|\alpha(s)\| \leq 1$, where $\|.\|$ is the usual Euclidean norm of vectors. Thus,

$$\max_{s \in I} |q(\mathbf{p}(s))| = \max_{s \in I} |(\mathbf{D}\mathbf{c})^T \alpha(s)| \tag{6}$$

$$\leq \|\mathbf{D}\mathbf{c}\| \max_{s \in \Omega} \|\alpha(s)\| \leq \|\mathbf{D}\mathbf{c}\|. \tag{7}$$

An approximate implicitization of the given curve can now be found by minimizing $\|\mathbf{D}\mathbf{c}\|$ subject to $\|\mathbf{c}\| = 1$. The latter constraint is needed in order to exclude the trivial solution.

The solution $\tilde{\mathbf{c}}$ can be found efficiently by performing a singular value decomposition (SVD) of $\mathbf{D}$ (see [16]) and choosing the singular vector corresponding to the smallest singular value $\sigma_{\min}$. This gives

$$\|\mathbf{D}\tilde{\mathbf{c}}\| \leq \sigma_{\min}.$$

Summing up, the approximate implicitization is defined by the bivariate polynomial $\tilde{q}$ with coefficient vector $\tilde{\mathbf{c}}$. This polynomial satisfies

$$\max_{s \in I} |\tilde{q}(\mathbf{p}(s))| \leq \sigma_{\min}. \tag{8}$$

This result possesses the following geometric interpretation: The given curve segment $\mathbf{p}(s)$ with $s \in I$ is contained in the "fat" algebraic curve

$$q^{-1}([-\sigma_{\min}, \sigma_{\min}]) \cap \Omega = \{\mathbf{x} \in \Omega : \; -\sigma_{\min} \leq q(\mathbf{x}) \leq \sigma_{\min}\}. \tag{9}$$

This region of the plane is bounded by the two algebraic offset curves $q(\mathbf{x}) = -\sigma_{\min}$ and $q(\mathbf{x}) = \sigma_{\min}$. In particular, if the matrix $\mathbf{D}$ possesses the singular value zero, then the corresponding singular vector gives the coefficients of an exact implicitization of the given rational curve.

As shown by Dokken, approximate implicitization possesses a high order of approximation. Thus, the error converges to zero very quickly if the length of the interval I is decreased. However, the method certainly only considers metric aspects. Additional considerations need to be taken into accounct to certify, that the approximate implicitization possesses the correct topology, cf. [26].

As a problem for the implementation and practical usage of approximate implicitization, the numerically stable computation of the matrix $\mathbf{D}$ in (4) is relatively complicated, requiring composition algorithms for polynomials in Bernstein-Bézier form. In addition, the number of entries grows quite fast with m. Also, the technique is not suitable for approximate implicitization by spline functions q, since the space of functions generated by the compositions $q \circ \mathbf{p}$ depends on the given curve and does not possess a simple basis.

2.2 Weak approximate implicitization

In order to avoid these computational difficulties, the weak method for approximate implicitization (cf. [9]) considers directly the basis $\beta(\mathbf{x})$, which was already introduced in (3), and integrates the squared residuals $q(\mathbf{p}(s))$ over the interval I,

$$\int_I q(\mathbf{p}(s))^2 \mathrm{d}s = \int_I \left(\mathbf{c}^T \beta(\mathbf{p}(s))\right)^2 \mathrm{d}s = \mathbf{c}^T \mathbf{M} \mathbf{c}, \tag{10}$$

with the symmetric matrix

$$\mathbf{M} = \int_I \beta(\mathbf{p}(s)) \beta(\mathbf{p}(s))^T \mathrm{d}s. \tag{11}$$

Clearly, one may use numerical methods for evaluating the integrals.

Note that the choice of the basis β depends on the region of interest Ω, which reflects the local character of the weak approach. For instance, one may consider the Bernstein-Bézier polynomials with respect to a triangle containing the region of interest.

The weak approximate implicitization of the given curve is found by minimizing the objective function defined in (10) subject to the constraint $\|\mathbf{c}\| = 1$. Similar to the original method, SVD can be used to find the solution $\tilde{q}$ with the coefficient vector $\tilde{\mathbf{c}}$. The value of (10) is equal to the smallest singular value $\sigma_{\min}$ of $\mathbf{M}$.

Since we are considering a compact interval I and the space of polynomials of degree mn defined on it, there exists a constant C (depending on the degree mn and on I, but not on the given curve) such that

$$\max_{s \in I} |\tilde{q}(\mathbf{p}(s))| = \|\tilde{q} \circ \mathbf{p}\|_\infty \leq C \|\tilde{q} \circ \mathbf{p}\|_2 = C\sqrt{\sigma_{\min}}, \tag{12}$$

where the norms $\|.\|_2$ and $\|.\|_\infty$ are the L^2 and the maximum norm of polynomials in I. Thus, the weak approximate implicitization admits a similar geometric interpretation as the original approach, cf. (9).

2.3 Interpolation constraints

Additional interpolation constraints, which force the approximate implicitization to match a certain number of given points, can be added either before or after the SVD.

Consider the first possibility. Suppose that we want our approximation to interpolate a point $\mathbf{p}_0$. Following the weak approach, this gives the condition

$$q(\mathbf{p}_0) = \mathbf{c}^T \beta(\mathbf{p}_0) = 0. \tag{13}$$

Using a Lagrangian multiplier, one is led to apply the SVD to the modified matrix

$$\tilde{\mathbf{M}} = \begin{pmatrix} \mathbf{M} & \beta(\mathbf{p}_0) \\ \beta(\mathbf{p}_0)^T & 0 \end{pmatrix}, \tag{14}$$

and then to omit the last entry of the singular vector.

As a second method, one may compute a linear combination of the singular vectors of **M** which are associated with the smallest singular values, in order to satisfy the interpolation condition(s). In the remainder of the paper we will use the first (Lagrange-multiplier-based) interpolation method.

3 Envelopes

The envelope of a family of curves is a curve which touches each member of the family. Following the approach in [22], we will use a spatial interpretation to describe this property. First we explain this in the case of an implicitly defined family of curves, and then we proceed to the case of parametric curves.

3.1 Implicitly defined curves

We consider a family of real, planar curves which are defined as the zero sets of a trivariate polynomial $F(\mathbf{p},t)$, where $\mathbf{p} = (p_1, p_2) \in \Omega \subset \mathbb{R}^2$ are the coordinates and $t \in J \subseteq \mathbb{R}$ is the time-like parameter identifying the members of the family. The domain Ω represents the region of interest, and the time-like parameter t varies in an interval $J \subset \mathbb{R}$. For each constant value $t = t_0$, the set of points satisfying $F(\mathbf{x},t_0) = 0$ forms a planar curve. As t varies in J, we obtain a one-parameter family of curves.

Let ∂_t denote the partial differentiation with respect to t. The envelope $\mathscr{D}$ of the family is defined as

$$\mathscr{D} = \{\mathbf{p} \in \Omega : \exists t \in J : F(\mathbf{p},t) = \partial_t F(\mathbf{p},t) = 0\}. \tag{15}$$

Note that the set $\mathscr{D}$ may be empty and that in this case no real part of the envelope exists.

This definition can be understood with the help of the following spatial interpretation, see Fig. 1. The equation $F(\mathbf{p},t) = 0$ defines a surface S in three-dimensional space with coordinates $\mathbf{p} = (p_1, p_2)$ and t. The intersections with the planes $t =$ constant, give – after projecting them orthogonally into the (p_1, p_2)-plane – the curves which belong to the family. We will denote this orthogonal projection by π.

The set of all points of the surface S satisfying $\partial_t F(\mathbf{x},t) = 0$ forms the *contour* with respect to the projection π, and their image is the *silhouette* of the surface. The tangent planes of the surface along the contours are projected into lines, since their normal vectors are perpendicular to the direction of projection.

For any point $\mathbf{P} = (\mathbf{p}, t_0)$ of the contour, we consider the intersection curve with the plane $t = t_0$ through this point. Both this curve and the contour touch the tangent plane at the point $\mathbf{P}$. Thus, the projections – which are the curve of the family and the envelope – possess the same tangent at $\mathbf{p} = \pi(\mathbf{P})$, which is obtained as the image of the tangent plane.

Therefore we can think of an envelope as the silhouette of a surface under π. The contour – which is projected into the silhouette – is defined as the intersection of the two surfaces $F = 0$ and $\partial_t F = 0$. The implicit equation of the envelope can be found by eliminating t from both equations.

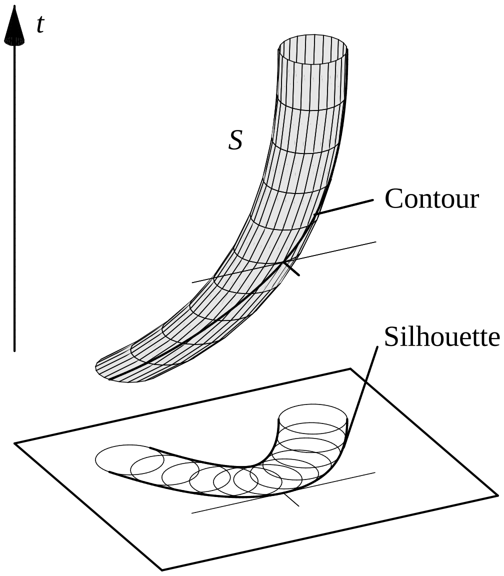

Figure 1: Spatial interpretation of envelopes: The contour of the surface S is projected into the silhouette. Simultaneously, this gives the envelope of the family of curves obtained by projecting the intersections of S with planes $t =$ constant into the (p_1, p_2)-plane.

3.2 Parametric curves

In this paper we are mainly interested in the case of a rational family of rational curves. More precisely, we consider a family of curves

$$\mathbf{p}(s,t) = \left(\frac{x(s,t)}{w(s,t)}, \frac{y(s,t)}{w(s,t)} \right)^T, \quad (s,t) \in I \times J \tag{16}$$

where x, y and w are bivariate polynomials of degree (n_1, n_2) with $\gcd(x,y,w) = 1$ and the domain is the Cartesian product of two closed intervals $I, J \subset \mathbb{R}$. We assume that $w(s,t) \neq 0$ for all $(s,t) \in I \times J$. For each constant value of the second (time-like) parameter $t = t_0$, we obtain a segment of a rational curve $s \mapsto \mathbf{p}(s,t_0)$ with domain I.

We consider the embedding

$$\tilde{\mathbf{p}}(s,t) = \left(\frac{x(s,t)}{w(s,t)}, \frac{y(s,t)}{w(s,t)}, t \right)^T \tag{17}$$

of the family of curves into the three-dimensional space with coordinates (p_1, p_2) and t.

In order to find an implicit equation of the envelope, one could proceed as follows: First one might compute a t-dependent implicit equation of the form $F(\mathbf{p},t) = 0$, i.e. an implicit equation of the surface $\tilde{\mathbf{p}}$. Second, one could derive the implicit equation as described in the previous section. This approach – which requires the elimination of three variables – is fairly complicated, and we prefer to work directly with the parametric representation.

As in the previous section, we are interested in the *contour* of the surface $\tilde{\mathbf{p}}$ with respect to the parallel projection π. The contour consists of all points whose normal vector is parallel to the (p_1, p_2)-plane. The third coordinate of the normal vectors $\partial_s \tilde{\mathbf{p}} \times \partial_t \tilde{\mathbf{p}}$ is the rational function $h(s,t)/w(s,t)^3$ with the numerator

$$h(s,t) = \det \begin{pmatrix} x(s,t) & \partial_s x(s,t) & \partial_t x(s,t) \\ y(s,t) & \partial_s y(s,t) & \partial_t y(s,t) \\ w(s,t) & \partial_s w(s,t) & \partial_t w(s,t) \end{pmatrix}. \tag{18}$$

The zero set $Z = h^{-1}(0)$ of this bivariate polynomial h defines the points in $I \times J$ which correspond to the envelope.

We will refer to $h(s,t)$ as the *envelope function* and to $h(s,t) = 0$ as the *envelope condition*. Note that h is independent of the choice of the third coordinate of $\tilde{\mathbf{p}}$, i.e. for any embedding of the form $(p_1, p_2, z(s,t))^T$ with an arbitrary function $z(s,t)$, the envelope function is the same. This is due to the fact that all these embeddings generate the same silhouette.

If a rational parameterization $(s(\xi), t(\xi))$ of the curve defined by $h(s,t) = 0$ were available, we could obtain a parametric description $\mathbf{k}(\xi)$ of the envelope by composing it with $\mathbf{p}$, $\mathbf{k}(\xi) = \mathbf{p}(s(\xi), t(\xi))$. However, the envelope condition does not define a rational curve in general.

The envelope function h equals the numerator of the Jacobian determinant of $\mathbf{p}$. Indeed, the envelope consist of the singular points of the mapping $\mathbf{p}$ (cf.[5]). Thus singularities of the specific parametrization are a part of the envelope and h necessarily depends on the parametrization.

4 Approximate implicitization of envelopes

We present a modification of weak approximate implicitization which is well suited for the computation of envelopes. More precisely, we consider the following problem.

Given a family of rational curves (16), find an approximate implicit representation of the envelope. Several possible approaches exist, which we list below.

1. One could implicitize the surface $\tilde{\mathbf{p}}(s,t)$ (see (17)) in order to obtain an implicit representation $F(\mathbf{p}, t) = 0$ of the family of curves. It is then possible to use the technique outlined in Section 3.1, i.e., to find the implicit equation of the envelope by eliminating t from $F = 0$ and $\partial_t F = 0$. Generally, the degree of F will be rather high, making this method impractical.

   Applying approximate implicitization to $\tilde{\mathbf{p}}$ is also inadequate, since one first has to compute a *surface* and then compute its contour to get the envelope *curve*.

2. Sometimes it may be possible to find a (rational) parameterization of the curve represented by the envelope condition $h(s,t) = 0$. By composing it with the parametric representation of the family of curves one then obtains a parametric representation of the envelope. This possibility is rather theoretical, since the curve $h(s,t) = 0$ can generally not be parameterized by elementary functions (in the sense of [29]) and it is generally not known how to generate such a parametrization, except for rational [27] or square-root parametrizations [30]. Also, this approach would give a parametric representation of the envelope, instead of an implicit one.

3. An implicit equation $q(\mathbf{x}) = 0$ of the envelope can also be derived directly by eliminating the parameters s, t, T from the four equations

   $$\{Xw(s,t) - x(s,t) = 0,\ Yw(s,t) - y(s,t) = 0,\ h(s,t) = 0, T\,w(s,t) = 1\}, \tag{19}$$

   where $\mathbf{x} = (X, Y)^T$. The last equation with the new variable T ensures that $w(s,t)$ does not vanish. We will present a special approximate technique for performing this elimination.

4.1 Jacobian embedding

Motivated by the system of equations (19), we define another embedding of the family of curves as

$$\hat{\mathbf{p}}(s,t) = \left(\frac{x(s,t)}{w(s,t)}, \frac{y(s,t)}{w(s,t)}, h(s,t) \right)^T. \tag{20}$$

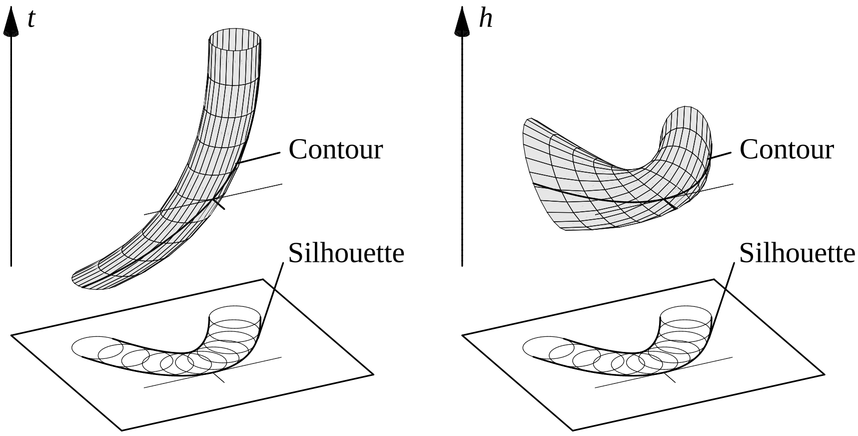

Figure 2: Transforming the embedding $\tilde{\mathbf{p}}$ (left) into the Jacobian embedding $\hat{\mathbf{p}}$ (right): The points on the contour are pushed into the plane, but the silhouette of the surface (which is simultaneously the envelope of the family of curves) remains the same.

We call it the *Jacobian embedding*, since the third coordinate is the numerator of the Jacobian determinant of the mapping $\mathbf{p}$.

By comparing this embedding with the spatial interpretation from section 3, one realizes that the Jacobian embedding possesses the same silhouette (envelope), since the envelope condition does not depend on the choice of the third coordinate. Moreover, all points that satisfy the envelope condition are embedded in the (p_1, p_2)-plane. Consequently, *the zero contour of the Jacobian embedding* $\hat{\mathbf{p}}$ *equals its silhouette*, hence the envelope.

As an example, Figure 2 shows the original embedding $\tilde{\mathbf{p}}$ of a family of curves and the Jacobian embedding $\hat{\mathbf{p}}$.

The (approximate) implicit equation $q(\mathbf{x}) = 0$ of the envelope could be found in the two steps of (1) (approximately) implicitizing the Jacobian embedding and (2) restricting the result to the points where the third coordinate is equal to zero. Consequently, the most direct approach is the use of approximate implicitization for finding a low degree approximation $\tilde{q}(\mathbf{x}, h)$ of the Jacobian embedding. The curve $\tilde{q}(\mathbf{x}, 0)$ gives an approximation of the envelope. However, this situation is similar to the approximate implicitization of $\tilde{\mathbf{p}}$. In order to find $\tilde{q}$, one has to compute an approximate implicitization of a *surface*, although we are only interested in the *curve* obtained as the intersection of that surface with the plane $h = 0$. Instead of this direct approach, we suggest to couple the envelope condition with the parametric representation in a different way, which is described in the next section.

4.2 Implicitization and the envelope function

When approximating the envelope of a rational family $\mathbf{p}$ with an algebraic curve $q = 0$, it is natural to consider their composition $q \circ \mathbf{p}$. Now there is a difference to the standard case of approximate implicitization: even for the exact equation of the envelope, we get $q(\mathbf{p}(s,t)) = 0$ only for specific values of s and t, which are determined by the envelope function h.

In this section, we consider the family of curves and its envelope in the complex affine plane $\mathbb{C}^2$. The envelope function possesses a factorization

$$h(s,t) = \prod_{i=1}^{M} h_i(s,t)^{k_i} \tag{21}$$

in $\mathbb{C}[s,t]$ with relatively prime, irreducible factors h_i and multiplicities $k_i \in \mathbb{Z}_+$. We say that h_i is a *proper* factor of the envelope function if the image of the algebraic curve $h_i(s,t) = 0$ – considered in the complex affine plane $\mathbb{C}^2$ – under the rational mapping $\mathbf{p}$ does not degenerate into a single point. Otherwise h_i is said to be *improper*.

Any *improper* factor h_i of the envelope function is characterized by the fact that the directional derivative of $\mathbf{p}$ along the tangent vectors of $h_i = 0$ is the null vector. Consequently, improper factors can be found in two steps. First one computes the squarefree representation

$$\hat{h}(s,t) = \prod_{i=1}^{M} h_i(s,t) \tag{22}$$

of the envelope function. Second, one finds the greatest common divisor of the two numerator polynomials in

$$-(\partial_t \hat{h})(\partial_s \mathbf{p}) + (\partial_s \hat{h})(\partial_t \mathbf{p}) \tag{23}$$

and the squarefree representation $\hat{h}$ of the envelope function. This gcd is the product of all improper factors.

We consider the *reduced envelope function*

$$\tilde{h}(s,t) = \prod_{\substack{i=1,\ldots,M \\ h_i \text{ is proper}}} h_i(s,t) \tag{24}$$

which is obtained by eliminating all improper factors and redundant powers of proper ones. The image of the algebraic curve $\tilde{h}(s,t) = 0$ under the rational mapping $\mathbf{p}$ is said to be the *proper part* of the envelope. Note that this may include complex components that were not considered in the previous discussion.

In addition to its proper part, the envelope consists of several (possibly complex) points, which are obtained as the images of the algebraic curves $h_i(s,t) = 0$ defined by improper factors under $\mathbf{p}$. These points are either contained in almost all curves of the family, or one of these curves degenerates into this single point. We illustrate the situation by a simple example.

Example 1 *We consider the family of circles through the point $(0,1)^T$ that touch the x-axis. It possesses the rational parameterization*

$$\mathbf{p} = \left(\frac{(s+t)(st+1)}{1+s^2}, \frac{s^2(1+t^2)}{1+s^2} \right)^T. \tag{25}$$

Its envelope function

$$h = (t+I)(t-I)s(1+st) \tag{26}$$

possesses the three improper factors $h_1 = t+I$, $h_2 = t-I$ and $h_4 = 1+st$. The algebraic curves $h_1 = h_2 = h_4 = 0$ are mapped to the three points $(I,0)$, $(-I,0)$ and $(0,1)$. The first two points are obtained as degenerate circles for $t = \pm I$, while the third point is contained in almost all circles. The only proper factor $\tilde{h} = h_3 = s$ is mapped to the envelope, which is the zero set of the linear polynomal $q(X,Y) = Y$. It satisfies

$$(q \circ \mathbf{p})(s,t)\, w(s,t) = (1+t^2)\, h_3(s,t)^2. \tag{27}$$

Therefore, the reduced envelope function appears with multiplicity 2 in $q \circ \mathbf{p}$.

We show that this observation is true in general:

Theorem 1 *Let* $\mathbf{p}(s,t) = \left(\frac{x(s,t)}{w(s,t)}, \frac{y(s,t)}{w(s,t)}\right)^T$ *be a rational family of planar rational curves, with* $w(s,t) \not\equiv 0$*. Let* $q(\mathbf{x}) = 0$ *be the square-free implicit equation of the proper part of the envelope and let* d *be its degree. There exists a bivariate polynomial* $g(s,t)$ *such that*

$$(q \circ \mathbf{p})(s,t)\, w(s,t)^d = g(s,t)\, \tilde{h}(s,t)^2.$$

Proof 1 *The proper part of the envelope consists of all points* $\mathbf{p}(s,t)$ *satisfying* $\tilde{h}(s,t) = 0$ *and* $w(s,t) \neq 0$*. Each proper factor* h_i *defines a (not necessarily real) component of the envelope. Since* $(q \circ \mathbf{p})(s,t)) = 0$ *holds for the infinite number of points satisfying* $h_i(s,t) = 0$*, we conclude that* h_i *is a factor of the numerator of* $q \circ \mathbf{p}$*.*

We show that h_i^2 *is a factor of the numerator of* $(q \circ \mathbf{p})$*, provided that* h_i *is proper. Since* h_i *is squarefree, it suffices to show that*

$$[\nabla_{st}(q \circ \mathbf{p})](s_0,t_0) = \mathbf{0} \tag{28}$$

for all points $(s_0,t_0) \in \mathbb{C}^2$ *satisfying* $h_i(s_0,t_0) = 0$*. Here* ∇_{st} *denotes the gradient with respect to* (s,t)*.*

Almost all points satisfying $h_i(s_0,t_0) = 0$ *are regular (i.e.* $(\nabla_{st} h_i)(s_0,t_0) \neq \mathbf{0}$*). We consider all points satisfying* $\partial_t h_i(s_0,t_0) \neq 0$*. Unless* $h_i(s,t)$ *is a scalar multiple of* $(t - t_0)$*, this covers almost all points on* $h_i(s_0,t_0) = 0$*. For each one of them, there exists a local regular parameterization* $\sigma \to (\sigma, t(\sigma))$*, where* σ *varies in a certain open neighborhood of* s_0 *in the complex plane* $\mathbb{C}$*. For almost all points among them, the correponding local parameterization of the envelope* $\sigma \mapsto \mathbf{p}(\sigma, t(\sigma))$ *is regular at* s_0*, i.e.*

$$\left(\frac{\mathrm{d}}{\mathrm{d}\sigma}\mathbf{p}(\sigma,t(\sigma))\right)(s_0) = (\partial_s \mathbf{p})(s_0,t_0) + (\partial_t \mathbf{p})(s_0,t_0)\, t'(s_0) \neq \mathbf{0}, \tag{29}$$

as the algebraic curve $h_i = 0$ *was assumed to be a proper component of the envelope function. Since the algebraic curve* $q = 0$ *covers all proper components of the envelope, we have that*

$$0 = \frac{\mathrm{d}}{\mathrm{d}\sigma}[q \circ \mathbf{p}(\sigma,t(\sigma))] = (\nabla_{xy} q)(\mathbf{p}(s_0,t_0)) \cdot [(\partial_s \mathbf{p})(s_0,t_0) + (\partial_t \mathbf{p})(s_0,t_0)\, t'(s_0)]. \tag{30}$$

On the one hand, the vector $(\partial_s \mathbf{p})(s_0,t_0) + (\partial_t \mathbf{p})(s_0,t_0) t'(s_0)$ *is not the null vector, since the parameterization was assumed to be regular* (29)*. On the other hand, the two vectors* $(\partial_s \mathbf{p})(s_0,t_0)$ *and* $(\partial_t \mathbf{p})(s_0,t_0)$ *are linearly dependent, as* $h(s_0,t_0) = 0$*. Consequently,*

$$0 = (\nabla_{xy} q)(\mathbf{p}(s_0,t_0)) \cdot (\partial_s \mathbf{p})(s_0,t_0) = (\nabla_{xy} q)(\mathbf{p}(s_0,t_0)) \cdot (\partial_t \mathbf{p})(s_0,t_0) \tag{31}$$

which implies (28)*. The case where* h_i *is a scalar multiple of* $t - t_0$ *can be dealt with similarly.*

This result admits the following simple geometric interpretation: Consider the Jacobian embedding $\hat{\mathbf{p}}$ along with the implicit equation of the envelope q. At regular intersection points with the plane $h = 0$, the tangent plane of this embedding is orthogonal to the plane $h = 0$. In three-dimensional XYh-space, the equation $q(X,Y) = 0$ defines a generalized cylinder which touches $\hat{\mathbf{p}}$ at all points in the plane $h = 0$, since the Jacobian embedding has vertical tangent planes there.

4.3 Coupled method for approximate implicitization of envelopes

Theorem 1 motivates us to find the approximate implicitization q of the envelope curve as an approximate solution of the equation

$$(q \circ \mathbf{p}) w^m = \lambda h^2, \tag{32}$$

where both q and λ are unknown. More precisely, λ is another polynomial in $(s,t) \in I \times J$, the free parameter m is the degree of q and w is the denominator of $\mathbf{p}$.

The polynomial q approximates the implicit equation of the envelope, while the auxiliary polynomial λ simultaneously approximates the factor g in theorem 1. We compute an approximate solution of (32) by minimizing the objective function

$$F = \int_{I\times J} \left(q(\mathbf{p}(s,t))w(s,t)^m - \lambda(s,t)h(s,t)^2\right)^2 \mathrm{d}(s,t), \tag{33}$$

that couples the composition $q \circ \mathbf{p}$ with the envelope function h. We will refer to λ as *coupling function*.

Let $q(\mathbf{x})$ be of degree m and $\lambda(s,t)$ of bidegree (k_1,k_2). After choosing bases $\alpha(s,t)$ and $\beta(\mathbf{x})$ of the bivariate polynomials of degree m and bidegree (k_1,k_2), respectively, we may represent the unknown polynomials as

$$q(\mathbf{x}) = \mathbf{c}_q^T \beta(\mathbf{x}) \quad \text{and} \quad \lambda(s,t) = \mathbf{c}_\lambda^T \alpha(s,t). \tag{34}$$

After substituting them into the objective function (33) we arrive at

$$F = \int_{I\times J} \left(\mathbf{c}^T\gamma\right)^2, \tag{35}$$

where

$$\mathbf{c} = \begin{pmatrix} \mathbf{c}_q \\ \mathbf{c}_\lambda \end{pmatrix} \quad \text{and} \quad \gamma = \begin{pmatrix} w(s,t)^m \beta(\mathbf{p}(s,t)) \\ -h(s,t)^2\alpha(s,t) \end{pmatrix}. \tag{36}$$

The minimizer of (35) subject to $\|\mathbf{c}\|_2 = 1$ can be found by applying SVD to the matrix

$$\mathbf{M} = \int_{I\times J} \gamma\gamma^T. \tag{37}$$

The first $(m+1)(m+2)/2$ entries of the solution vector are the coefficients of the approximating curve $q = 0$. Interpolation conditions (e.g., interpolation of points) can be incorporated by introducing constraints on this part of the solution.

Theorem 2 *Consider the rational family* (16) *of rational curves. We assume that the denominator w satisfies $|w(s,t)| \geq \varepsilon$ for a positive constant ε, for all $(s,t) \in I \times J$. Let $\tilde{\mathbf{c}}$ be the unit vector which corresponds to the smallest singular value σ_{min} of $\mathbf{M}$, $\tilde{q} = 0$ be the corresponding algebraic curve and $\tilde{\lambda}$ be the coupling function, respectively. We consider the envelope function h and its zero set*

$$\mathscr{H} = \{(s,t) \in I \times J : \ h(s,t) = 0\}.$$

Then

$$\max_{(s,t)\in\mathscr{H}} |\tilde{q}(\mathbf{p}(s,t))| \leq C\sqrt{\sigma_{min}},$$

where C is a positive constant which depends only on ε, I, J and on the degrees of $\mathbf{p}$, q and λ.

Proof 2 *For any compact set S and any function $f : S \to \mathbb{R}$, let $\|f\|_{\infty,S}$ be the supremum of f on S. Due to $|w(s,t)| \geq \varepsilon > 0$ we have in particular,*

$$\max_{(s,t)\in\mathscr{H}} |\tilde{q}(\mathbf{p}(s,t))| = \|\tilde{q} \circ \mathbf{p}\|_{\infty,\mathscr{H}}. \tag{38}$$

and moreover, there exists a positive constant $\tilde{C} \in \mathbb{R}$ such that

$$\|w^{-m}\|_{\infty,\mathscr{H}} \leq \tilde{C}. \tag{39}$$

This leads to

$$\begin{aligned} \|\tilde{q} \circ \mathbf{p}\|_{\infty,\mathscr{H}} &= \|(\tilde{q} \circ \mathbf{p}) w^m w^{-m}\|_{\infty,\mathscr{H}} \leq \|w^{-m}\|_{\infty,\mathscr{H}} \|(\tilde{q} \circ \mathbf{p}) w^m\|_{\infty,\mathscr{H}} \\ &\leq \tilde{C}\, \|(\tilde{q} \circ \mathbf{p}) w^m\|_{\infty,\mathscr{H}}. \end{aligned} \tag{40}$$

Recall that $\mathscr{H} \subset I \times J$ and $\|h\|_{\infty,\mathscr{H}} = 0$. Therefore

$$\|(\tilde{q} \circ \mathbf{p}) w^m\|_{\infty,\mathscr{H}} = \|(\tilde{q} \circ \mathbf{p}) w^m - \tilde{\lambda} h^2\|_{\infty,\mathscr{H}} \leq \|(\tilde{q} \circ \mathbf{p}) w^m - \tilde{\lambda} h^2\|_{\infty,I\times J}. \tag{41}$$

Since $I \times J$ is compact, there exists a positive constant $\hat{C} \in \mathbb{R}$ which depends solely on the degrees of the polynomials q, $\mathbf{p}$, λ and on the intervals I, J, such that

$$\|(\tilde{q} \circ \mathbf{p}) w^m - \tilde{\lambda} h^2\|_{\infty,I\times J} \leq \hat{C}\, \|(\tilde{q} \circ \mathbf{p}) w^m - \tilde{\lambda} h^2\|_{2,I\times J}, \tag{42}$$

where $\|.\|_{2,I\times J}$ is the L_2 norm of a function on $I \times J$. Since $\tilde{\mathbf{c}}$ minimizes (35),

$$(\|(\tilde{q} \circ \mathbf{p}) w^m - \tilde{\lambda} h^2\|_{2,I\times J})^2 = \sigma_{min}. \tag{43}$$

Combining (38) *and* (40)–(43) *we get*

$$\max_{(s,t)\in\mathscr{H}} |\tilde{q}(\mathbf{p}(s,t))| = \|\tilde{q} \circ \mathbf{p}\|_{\infty,\mathscr{H}} \leq C\sqrt{\sigma_{min}}, \tag{44}$$

where $C \in \mathbb{R}$ is a positive constant depending on ε, I, J and the degrees of $\mathbf{p}, \tilde{q}, \tilde{\lambda}$.

Thus, *all points of the envelope are contained in an algebraic offset of the approximating curve.* This geometric interpretation of the result is analogous to the case of weak approximate implicitization.

We demonstrate the performance of our method by a first example.

Example 2 *Consider the family of curves which is shown in Fig. 3. This is a family of bidegree $(1,3)$ and the exact envelope is an algebraic curve of degree 10. The family of lines $\mathbf{p}$ has been derived by slightly perturbing the coefficients of the family of tangents of a planar cubic.*

Fig. 4 shows the results of two approximate implicitizations with conics ($m = 2$) and cubics ($m = 3$). In both cases we used bilinear coupling functions. Note that the exact solution (dashed curve) possesses a self-intersection, which is not reproduced by the low-degree approximate solutions.

5 Piecewise approximate implicitization of envelopes

In principle, the presented method is capable of computing the exact implicit equation of the envelope. However, the degrees needed for that are generally rather large. For example, if the family $\mathbf{p}$ is described by a bivariate, quadratic polynomial, then the envelope function h is in the generic case of bidegree $(3,3)$. Thus the implicit equation of the Jacobian embedding can have a maximal degree $2\cdot 3\cdot 3 = 18$ and the same is true for the implicit equation of the envelope. Since we want to satisfy $q \circ \mathbf{p} = \lambda h^2$, both degrees of the coupling function λ need to be $2\cdot 18 - 2\cdot 3 = 30$.

In total we get $\frac{1}{2}(19\cdot 20) + 31^2 = 1151$ degrees of freedom. Solving such a high degree problem is computationally expensive, since it requires the construction and SVD of a 1151×1151 matrix. For practical purposes, a piecewise approximation by low degree curves is more useful.

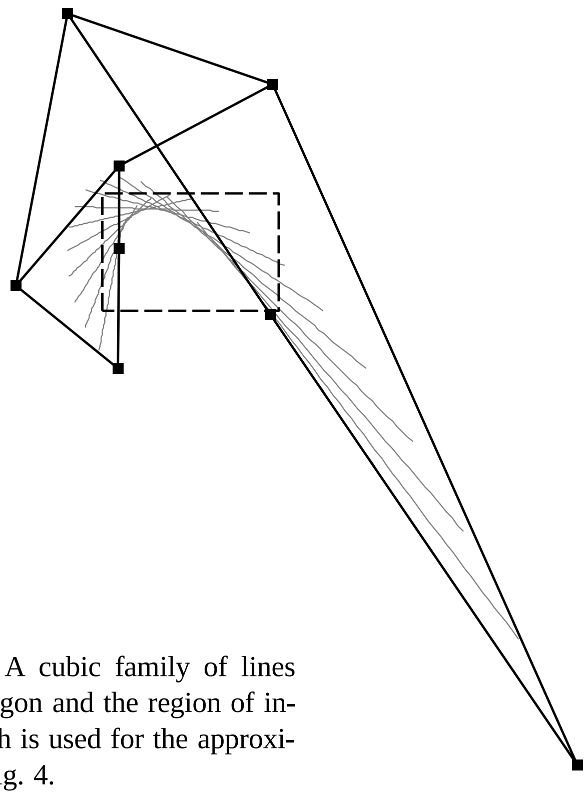

Figure 3: Example 2. A cubic family of lines (grey), their control polygon and the region of interest (dashed box) which is used for the approximate implicitization in Fig. 4.

5.1 The Algorithm

As before, we are considering a (rational) family of rational curves (cf. (16)). Without loss of generality we can assume that $I \times J = [0,1] \times [0,1]$. Let the degrees of $\mathbf{p}$ be (n_1, n_2). We describe $\mathbf{p}$ in Bernstein-Bézier representation:

$$\mathbf{p}(s,t) = \frac{\sum_{i,j} \mathbf{p}_{ij} w_{ij} B_i^{n_1}(s) B_j^{n_2}(t)}{\sum_{i,j} w_{ij} B_i^{n_1}(s) B_j^{n_2}(t)}, \tag{45}$$

with $B_k^n(z) = \binom{n}{k}(1-z)^k z^{n-k}$ and $\mathbf{p}_{ij} \in \mathbb{R}^2, w_{ij} \in \mathbb{R}, 0 \le i \le n_1, 0 \le j \le n_2$.

We formulate an algorithm which computes an approximation of the envelope curve by pieces of algebraic curves. The segments of the curves are joined continuously at their end points. Moreover, if the envelope curve possesses different branches in the region of interest, then all of them will be approximated.

The algorithm is based on two assumptions on h:

(i) The envelope function h is squarefree and does not possess improper factors.

(ii) The zero set of h has no singularities in $I \times J$.

The first assumption is needed for the stability of the numerical computations, which are performed by using floating point numbers, and in order to use Theorem 1. If improper factors are present, then the algorithm can still be executed, but it may not give optimal results.

As a possible extension of our approach, one might use a factorization of h and gcd computations in order to identify the reduced envelope function $\tilde{h}$. This extension, however, requires special techniques for polynomials with coefficients given by floating point numbers, cf. [15]. The degree of the

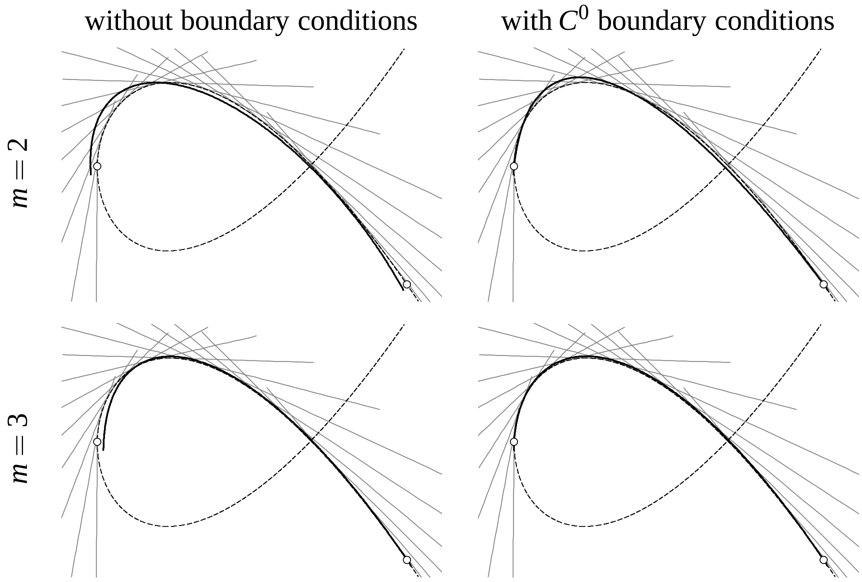

Figure 4: Example 2. Approximate implicitization of the family of lines from Fig. 3. In addition to the family of curves (grey), the figure shows approximations of the envelopes for degrees $m = 2,3$ and $(k_1,k_2) = (1,1)$ (black, solid) and the exact envelopes (dashed). The circles mark the segment end points of the envelope in the region of interest. The curves in the right column interpolate these points.

approximation segments and the degrees of the coupling functions are the free parameters. We denote them with m and (k_1,k_2), respectively.

The main idea of the approach is a recursive subdivision of the parameter domain $I \times J$ into four (squared) subdomains. We use a minimum recursion depth $r \geq 0$ in order to control the detection of small closed loops which may be part of the envelope. Thus, each box in the parameter domain which contains a part of the zero set of h has at most a diameter of $2^{-r}\sqrt{2}$.

The algorithm consists of four steps:

1.) Compute the Bernstein-Bézier representation of the envelope function, denoting its coefficient matrix with H.

2.) If the entries of H are either all positive or all negative, then no envelope exists in this domain (convex hull property) and the algorithm terminates. Otherwise continue with step 3.

3.) Compute all real intersection points (s_l,t_l) of $h(s,t) = 0$ with the boundaries of the considered domain. Collect the coordinates $\mathbf{p}(s_l,t_l)$ in a set $\mathscr{S}$.

4.) If $|\mathscr{S}| = 2$ and $r \leq 0$ compute an approximate implicitization of the envelope, interpolating the points in $\mathscr{S}$ and using degrees m and (k_1,k_2) (cf. Section 4.3). Otherwise, subdivide p into four parts and apply the algorithm to each of them, using $r-1$ as their minimum recursion depth.

In our current implementation, the computation in step 3 is performed numerically. Alternatively one might be using Sturm sequences or the variation diminishing property of the Bernstein-Bézier representation of h to certify the number of intersections.

5.2 Discussion

The recursive subdivision stops, if after at least r steps exactly two solutions of $h = 0$ are found on the boundary of the currently considered parameter domain. Due to the previous assumptions on h, the algorithm always terminates in the generic case. Problems may occur if the zero set of h incidentally touches one of the boundaries of the boxes generated by the subdivision. In the generic case this does not occur.

We aim to approximate always just one (part of a) branch of the envelope with one algebraic curve. If closed loops of the zero set of h are contained in one subdomain, then each of them contributes an additional branch to the envelope. Since we perform at least r subdivision steps, all loops with a diameter which is bigger than $2^{-r}\sqrt{2}$ are found. Loop detection is a well known problem and has been extensively studied (see for example [20]).

There is no special treatment of singularities of the envelope. Usually, after some subdivisions, the approximation interpolates at least one point close to the singularity. The segments are connected at these points and their C_0-transition mimics the behavior of a cusp point.

In order to bound the region of each segment generated by the approximate implicitization, we use the convex hull of the control points which correspond to the associated box in the parameter domain. These convex hulls necessarily intersect each other. An example of this behavior is given in Fig. 5. It shows some segments of an approximation of the family from Fig. 3. The domains of these segments intersect themselves in a quite large area and thus introduce some ambiguity. However, this can often be resolved by analyzing the location of the segment end points.

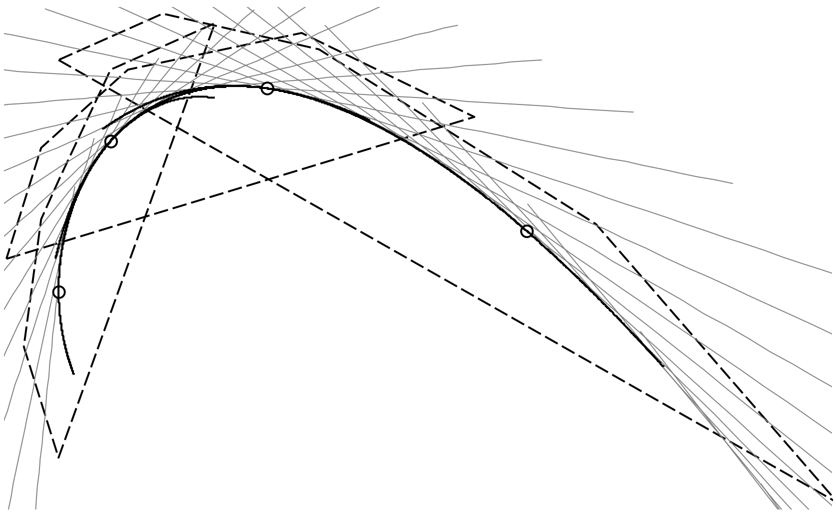

Figure 5: Piecewise approximation of a part of the family from Fig. 3 (grey). Three approximating segments (black, solid) and their domains (black, dashed) are shown. Each domain contains two associated interpolation points (circles) and the relevant part of their segment is the arc in between them. In order to improve the visibility, each of the three arcs have been extrapolated slightly beyond its boundary points.

In addition, by repeating the first two steps of the algorithm – without further approximation – we can identify smaller domains for each segment. This decreases the area of mutual intersection. In a final step, we can use the control net of the Jacobian embedding for each part of the parameter domain. The projection of this control net to the plane $z = 0$ exactly gives the control net of the corresponding part of the parameter domain. Now we compute the three-dimensional convex hull $\mathrm{CH}(\hat{\mathbf{p}})$ of the control net of the Jacobian embedding. Due to its definition, all points of the envelope must be contained in the intersection of $\mathrm{CH}(\hat{\mathbf{p}})$ with the plane $z = 0$. This reduces the domain for each approximating segment even further.

It may happen that single segments of the approximation consist of unconnected branches. So far, no part of the algorithm prohibits an approximation with separate branches. In our experience the unconnected, interpolating segments typically get connected after some subdivision steps. However, this issue is a common feature of most methods for approximate implicitization.

The values for k_1, k_2 should depend on the value of m and a good choice for them is hard to make in general. However, so far we experienced $k_1 = k_2 = m$ giving good results in our test cases.

5.3 Examples

We will illustrate the performance of the algorithm by several examples. The algebraic curves were plotted via a predictor-corrector method, using the interpolation points (circles) as initial values.

Example 3 *Offsets of a parabola. If the distance is chosen high enough, the offset of a parabola contains a "swallowtail" in one of its branches. This part of the offset contains two cusps and one self-intersection. In Fig. 6, the relevant part of an offset and approximations with conics of different subdivision levels are depicted. Furthermore, the corresponding parameter domains are shown to illustrate the subdivision process.*

Example 4 *WV-shaped curve. We used cubic splines and cubic coupling functions to approximate a rational family of rational curves of bidegree* $(3,2)$ *(see Fig. 7). The subdivision clearly improves the reproduction of singularities and gives connected segments.*

Example 5 *Closed curve with cusps. Closed loops of the envelope may possess several cusps - Fig. 8 shows such an example. The considered rational family of curves is of bidegree* $(2,2)$ *and quadratic splines and coupling functions were used for the envelope approximation.*

Example 6 *Envelope of circles. We approximated the envelope of a medial axis transformation. Two rational functions of bidegree* $(5,3)$ *described the family of circles. Conic sections and bivariate, quadratic coupling functions were used (see Fig. 9).*

6 Conclusions

We have shown that approximate implicitization can be adapted to compute the envelope of a family of curves. Additionally we described an algorithm for computing a piecewise approximation of the envelope with algebraic curves of chosen degree. The numerical examples show that approximate implicitization is well suited for the computation of envelope curves.

As a topic for future work, we will analyze the approximation order of the curves generated by approximate implicitization of envelopes. Furthermore, we are currently working on an extension to envelope surfaces.

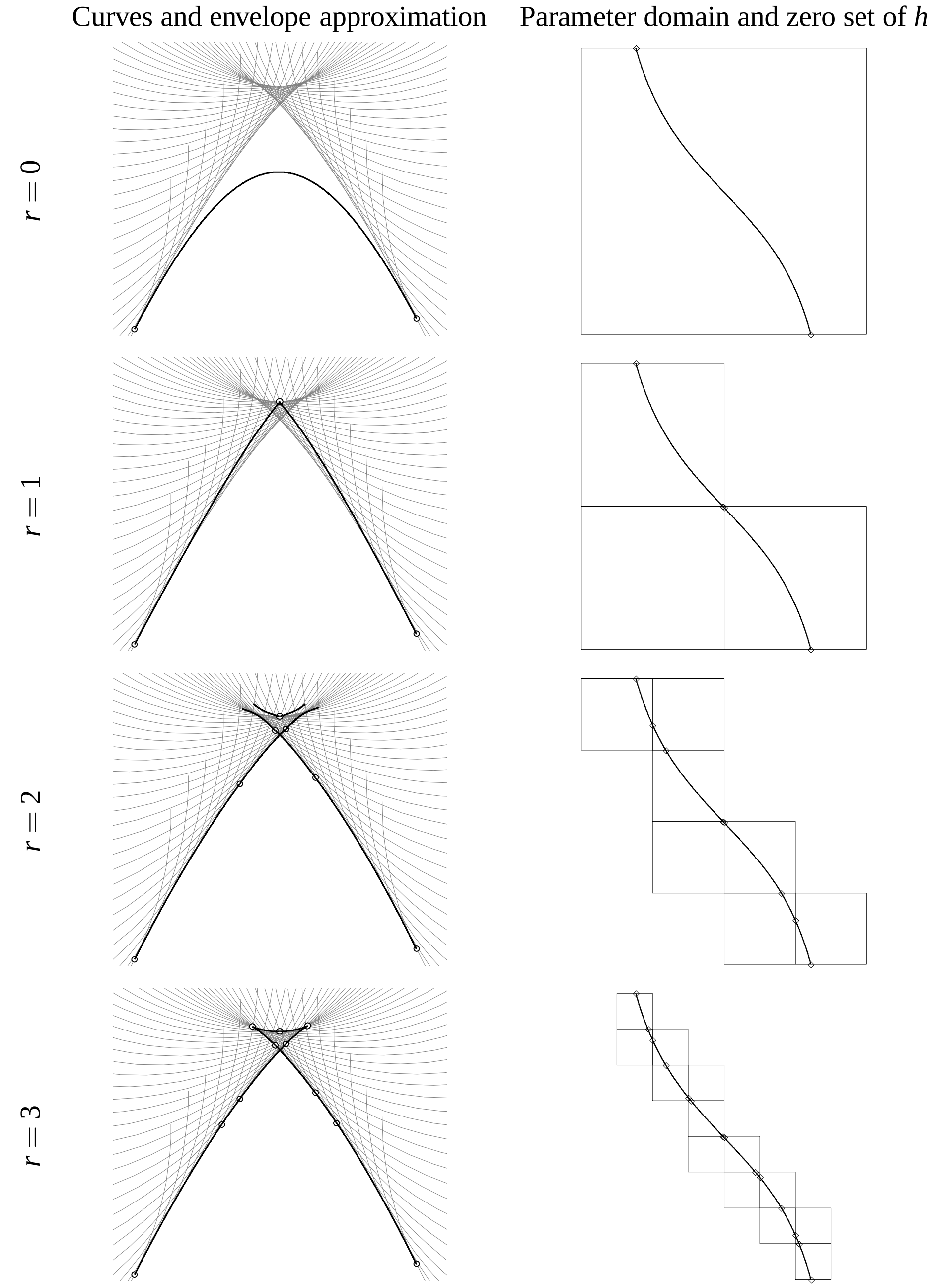

Figure 6: Example 3. Approximation of an offset of a parabola. The family of curves consists of circular arcs with constant radius, which are centered along a parabola. In each row a piecewise approximation with conics ($m = 2$,$(k_1, k_2) = (2, 2)$) and their corresponding parameter domains are shown. In addition, the zero set of the envelope function is plotted. Each circle on the left side is interpolated and corresponds to a diamond on the right. The minimum recursion depth is $r = 0, 1, 2, 3$, respectively.

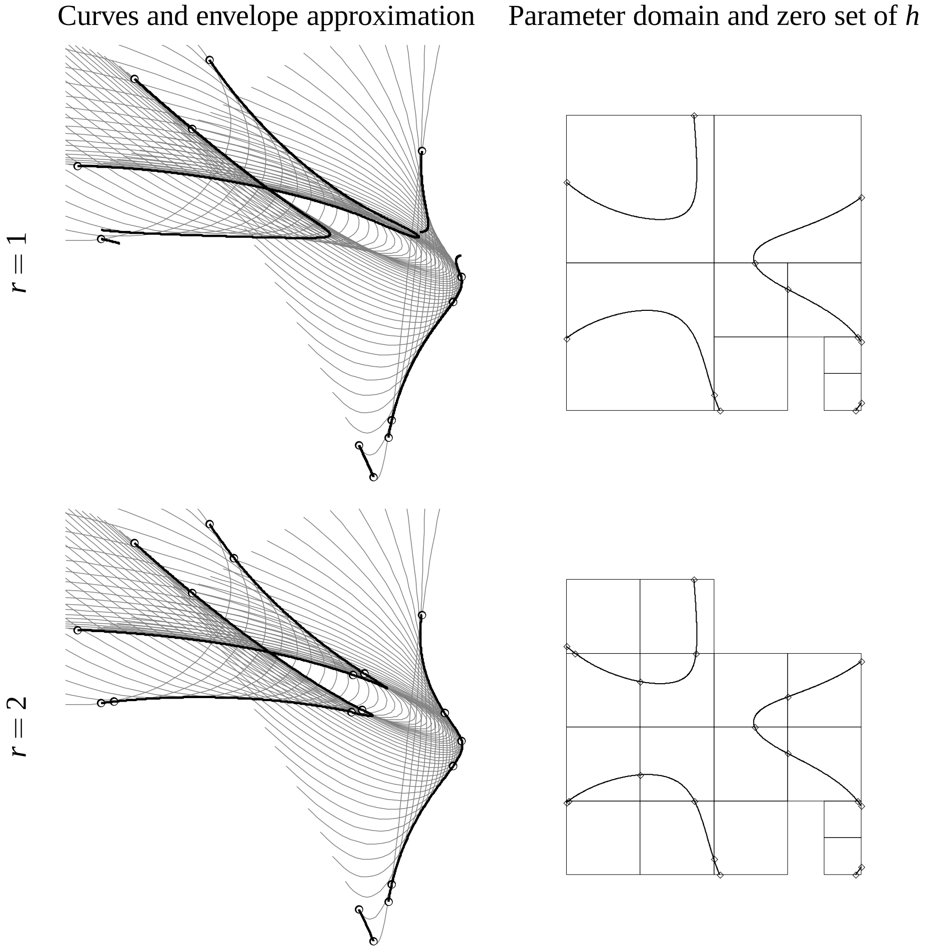

Figure 7: Example 4. Approximate implicitization of an envelope curve consisting of several branches with cubic curves ($m = 3$, $(k_1, k_2) = (3, 3)$). The right side shows the corresponding parameter domains and the zero set of the envelope function. Each branch of this curve gives one branch of the envelope. First row ($r = 1$): Several segments are unconnected and the singularities are not reproduced properly. Second row ($r = 2$): Further subdivision gives connected segments and an improved approximation of the singularities.

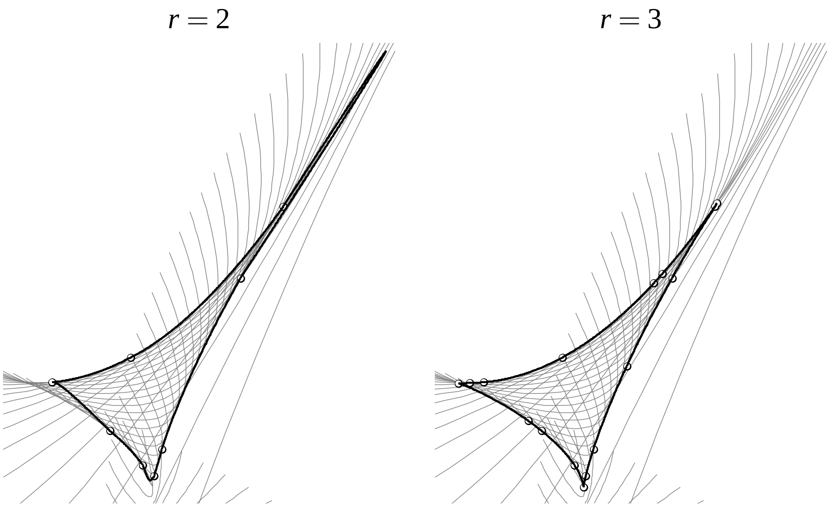

Figure 8: Example 5. Loops of envelopes usually contain several cusps. In this example the degrees were $m = 2$ and $(k_1, k_2) = (2, 2)$, so the segments cannot contain singularities. Left ($r = 2$): The cusps are not represented very well, since the segment end points are too far away. Right ($r = 3$): After an additional subdivision step some segment end points are close to the cusps, so that the singularities are approximated well.

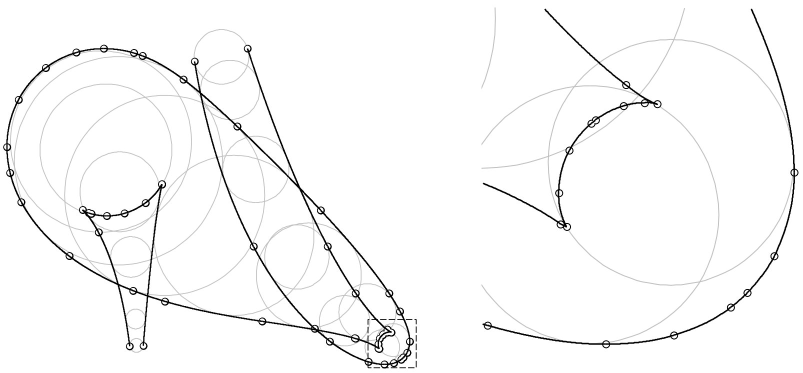

Figure 9: Example 6. Piecewise approximation of the envelope generated by a medial axis transformation with 53 segments using the degrees $m = 2$ and $(k_1, k_2) = (2, 2)$. The right picture shows a enlarged version of the dashed region in the left one. Note the dense distribution of interpolation points near the singularities.

Acknowledgments. This research has been supported by the Austrian Science Fund (FWF) in the frame of the FSP S092 “Industrial Geometry”, subproject 2. The authors would like to thank Josef Schicho and the referees for their useful comments which have helped to improve the manuscript.

References

[1] K. Abdel-Malek, J. Yang, D. Blackmore, and K. Joy. Swept volumes: fundation, perspectives, and applications. *International Journal of Shape Modeling*, 12(1):87–127, 2006.

[2] J. Alcazar. Good global behavior of offsets to plane algebraic curves. *Journal of Symbolic Computation*, 43(9):659–680, 2008.

[3] J. Alcazar, J. Schicho, and J. Sendra. A delineability-based method for computing critical sets of algebraic surfaces. *Journal of Symbolic Computation*, 42(6):678–691, 2007.

[4] J. Alcazar and J. Sendra. Local shape of offsets to algebraic curves. *Journal of Symbolic Computation*, 42(3):338–351, 2007.

[5] V. Arnold, S. Gusein-Zade, and A. Varchenko. *Singularities of differentiable maps*. Springer, 1985.

[6] C. Bajaj. The emergence of algebraic curves and surfaces in geometric design. *Directions in Geometric Computing*, pages 1–28, 1993.

[7] O. Bottema and B. Roth. *Theoretical Kinematics*. Dover Publications, 1990.

[8] T. Dokken. Approximate implicitization. *Mathematical methods for curves and surfaces, Oslo 2000*, pages 81–102, 2001.

[9] T. Dokken, H. Kellermann, and C. Tegnander. An approach to weak approximation implicitization. *Mathematical Methods for curves and surfaces, Oslo 2000*, pages 103–112, 2001.

[10] T. Dokken and J. Thomassen. Overview of approximate implicitization. In *Topics in Algebraic Geometry and Geometric Modeling: Workshop on Algebraic Geometry and Geometric Modeling, July 29-August 2, 2002, Vilnius University, Lithuania*, volume 334, pages 169–184. American Mathematical Society, 2003.

[11] T. Dokken and J. Thomassen. Weak approximate implicitization. In *IEEE International Conference on Shape Modeling and Applications, 2006. SMI 2006*, pages 204–214, 2006.

[12] M. Elkadi and B. Mourrain. Residue and implicitization problem for rational surfaces. *Applicable Algebra in Engineering, Communication and Computing*, 14(5):361–379, 2004.

[13] R. Farouki. *Pythagorean-Hodograph Curves: Algebra and Geometry Inseparable*. Springer, 2008.

[14] J. Flaquer, G. Garate, and M. Pargada. Envelopes of moving quadric surfaces. *Computer Aided Geometric Design*, 9(4):299–312, 1992.

[15] A. Galligo and M. van Hoeij. Approximate bivariate factorization: a geometric viewpoint. In *Proc. Int. Workshop on Symbolic-Numeric Computation*, pages 1–10. ACM, 2007.

[16] G. Golub and C. Van Loan. *Matrix computations*. The Johns Hopkins University Press, 1996.

[17] C. Hoffmann. Implicit curves and surfaces in cagd. *IEEE Computer Graphics and Applications*, 13(1):79–88, 1993.

[18] Y. Kim, G. Varadhan, M. Lin, and D. Manocha. Fast swept volume approximation of complex polyhedral models. *Computer-Aided Design*, 36(11):1013–1027, 2004.

[19] E. Kreyszig. *Differential Geometry*. Dover, 1991.

[20] N. Patrikalakis and T. Maekawa. *Shape interrogation for computer aided design and manufacturing*. Springer Verlag, 2002.

[21] M. Peternell, H. Pottmann, T. Steiner, and H. Zhao. Swept volumes. *Computer-Aided Design Appl*, 2:599–608, 2005.

[22] H. Pottmann and M. Peternell. Envelopes-computational theory and applications. In *Spring Conference on Computer Graphics*, pages 3–23. Comenius University, Bratislava, 2000.

[23] M. Rabl, B. Jüttler, and L. Gonzalez-Vega. Exact envelope computation for moving surfaces with quadratic support functions. In Lenarcic and Wenger, editors, *Advances in Robot Kinematics: Analysis and Design*, pages 283 – 290. Springer, 2008.

[24] F. San Segundo and J. Sendra. Partial degree formulae for plane offset curves. *Journal of Symbolic Computation*, 44(6):635–654, 2009.

[25] T. Sederberg. Planar piecewise algebraic curves. *Computer Aided Geometric Design*, 1(3):241–255, 1984.

[26] T. Sederberg, J. Zheng, K. Klimaszewski, and T. Dokken. Approximate implicitization using monoid curves and surfaces. *Graphical Models and Image Processing*, 61(4):177–198, 1999.

[27] J. Sendra, F. Winkler, and S. Perez-Diaz. *Rational algebraic curves*. Springer, 2007.

[28] M. Shalaby, J. Thomassen, E. Wurm, T. Dokken, and B. Jüttler. Piecewise approximate implicitization: Experiments using industrial data. In B. Mourrain, M. Elkadi, and R. Piene, editors, *Algebraic Geometry and Geometric Modeling*, pages 37–52. Springer, 2006.

[29] D. Shanks. *Solved and unsolved problems in number theory*. AMS Chelsea Pub., 1993.

[30] M. Van Hoeij. An algorithm for computing the Weierstrass normal form. In *Proc. Int. Symp. Symbolic and Algebraic Computation*, pages 90–95. ACM, 1995.

[31] E. Wurm, J. Thomassen, B. Jüttler, and T. Dokken. Comparative benchmarking of methods for approximate implicitization. In M. Neamtu and M. Lucian, editors, *Geometric Modeling and Computing: Seattle 2003*, pages 537–548. Nashboro Press, Brentwood, 2004.